



Parameter Optimization of Multi-element Synthetic Aperture Imaging Systems

Vera Behar

*Institute for Parallel Processing – Bulgarian Academy of Sciences
25-A Acad. G. Bonchev Str., Sofia 1113, Bulgaria
E-mail: behar@bas.bg*

Received: January 19, 2007

Accepted: Mart 16, 2007

Published: Mart 27, 2007

Abstract: *In conventional ultrasound imaging systems with phased arrays, the further improvement of lateral resolution requires enlarging of the number of array elements that in turn increases both, the complexity and the cost, of imaging systems. Multi-element synthetic aperture focusing (MSAF) systems are a very good alternative to conventional systems with phased arrays. The benefit of the synthetic aperture is in reduction of the system complexity, cost and acquisition time. In a MSAF system considered in the paper, a group of elements transmit and receive signals simultaneously, and the transmit beam is defocused to emulate a single element response. The echo received at each element of a receive sub-aperture is recorded in the computer memory. The process of transmission/reception is repeated for all positions of a transmit sub-aperture. All the data recordings associated with each corresponding pair “transmit-receive sub-aperture” are then focused synthetically producing a low-resolution image. The final high-resolution image is formed by summing of the all low-resolution images associated with transmit/receive sub-apertures. A problem of parameter optimization of a MSAF system is considered in this paper. The quality of imaging (lateral resolution and contrast) is expressed in terms of the beam characteristics – beam width and side lobe level. The comparison between the MSAF system described in the paper and an equivalent conventional phased array system shows that the MSAF system acquires images of equivalent quality much faster using only a small part of the power per image.*

Keywords: *Ultrasound imaging, Synthetic aperture design, Parameter optimization, Simulation analysis.*

Introduction

Images produced by ultrasound imaging systems must be of sufficient quality in order to provide accurate clinical interpretation. The image quality (lateral resolution and contrast) is primarily determined by the beam characteristics of a transducer used in an imaging system. In conventional ultrasound imaging systems with phased array (PA), all transducer elements transmit signals and receive the echoes, reflected from the tissue. Thus the modern conventional PA systems produce high-resolution images at high cost because the system complexity and thus the system cost depend on the number of transducer elements. The further improvement of lateral resolution in a conventional PA imaging system requires enlarging of the number of transducer elements. It is often not possible because of physical constraints or too high cost. The effect of high lateral resolution and contrast can be accomplished by using various synthetic aperture techniques. The benefit of the synthetic aperture is in reduction of the system complexity and cost. Moreover, in a synthetic aperture imaging system, the acquisition time can be drastically reduced and the dynamical steering and focusing can be applied in both transmit and receive. There are different methods for synthetic aperture imaging – *Synthetic Receive Aperture (SRA)* technique, *Synthetic Transmit Aperture (STA)* technique, *Synthetic Aperture Focusing (SAF)* technique, and *Multi-Element Synthetic Aperture Focusing (MSAF)* technique.

In the PA imaging, the image acquisition time is evaluated as $T_{PA} = T_{REC} \cdot N_{line}$, where T_{REC} is the time needed to acquire RF-signals at a single scan direction, N_{line} is the number of all scan directions (number of image lines).

In the SRA imaging, a larger number of transducer receive elements is addressed without the same number of parallel receive channels [7, 8]. The SRA imaging technique involves transmitting with a full transmit aperture and receiving with several receive sub-apertures. It means that several pulse transmissions are needed to acquire a single RF line. The image acquisition time is evaluated as $T_{SRA} = M \cdot T_{REC} \cdot N_{line}$, where M is the number of transmissions. It is increased M times compared to the image acquisition time of a PA imaging system.

In the STA imaging, at each time one array element transmits an ultrasound pulse and all transducer elements receive the echoes [1, 9, 10]. The transducer elements are fired consequently, one after the other, and the echo signals received at each transducer element are stored in the computer memory. When the signals received from each pair “transmitter-receiver” have been recorded, a STA image is reconstructed by the appropriate algorithm. The time needed to acquire each STA image is evaluated as $T_{STA} = T_{REC} \cdot N$, where N is the number of array elements. The image acquisition time is reduced (N_{line} / N) times compared to an equivalent PA imaging system because as a rule $N_{line} > N$. The disadvantage is a huge data memory required to store N^2 RF-lines in order to produce a STA image.

In the SAF imaging, each transducer element acts as both transmitter and receiver [11, 12]. The full synthetic aperture is synthesized after all (N) array elements have transmitted and received the signals. The image acquisition time is evaluated as $T_{SAF} = T_{REC} \cdot N$. The image acquisition time is reduced (N_{line} / N) times compared to an equivalent PA imaging system. The system complexity is drastically reduced because the circuitry for only one pair “transmitter -receiver” is required. The Signal-to-Noise ratio (SNR), however, is reduced N^2 times compared to an equivalent PA imaging system.

In the MSAF imaging, in the transmit mode, a group of N_t elements transmit signals simultaneously, and the transmit beam is defocused to emulate a single element response [2, 3, 4, 5]. In the receive mode, a group of N_r elements receive the echo signals. The acoustic power and therefore the SNR are increased compared to the SAF imaging where a single transducer element is used in transmit. The image acquisition time is evaluated as $T_{MSAF} = M \cdot T_{REC}$, where M is the number of transmissions. The image acquisition time is reduced (N_{line} / M) times compared to an equivalent PA imaging system. When $M \ll N_{line}$, the reduction in acquisition time can be sufficiently large. A variant of the MSAF imaging, where only one element ($L = 1$) is dropped at the next transmission, is considered in [5]. In this system, a large number of pulse transmissions ($M \gg 1$) must be employed in order to obtain a high-resolution image because the number of elements used in a receive sub-aperture is very small ($N_r = 5$).

In general, the image quality produced by a MSAF imaging system is primarily determined by the following system parameters – the number of transmissions (M), the number of elements in a transmit sub-aperture (N_t), the number of elements in a receive sub-aperture (N_r), and

the number of elements (L) dropped at the next transmission. In most medical applications, the image acquisition time is required to be minimized in order to avoid the phase errors caused by tissue motion during the data acquisition. In order to satisfy this requirement, only a few pulse transmissions should be used for MSAF image formation ($M = 3, 5, 7$). When the number of transmissions is preset, it is very important to find the optimal combination of the other synthetic aperture parameters (L, N_r and N_t) in order to guarantee the needed quality of imaging.

In this paper, the parameter optimization of a MSAF system, in which the number of transmissions per image formation is small, is described. The system parameters N_r, M, N_t and L are optimized using the effective aperture concept for beam pattern analysis. The image quality (lateral resolution and contrast) is expressed in terms of the two-way beam pattern characteristics – beam width and side lobe level. The influence of sampling rate of RF signals on the image quality is also investigated. The comparison analysis between a 79-element MSAF system and an equivalent 79-element PA system shows that the MSAF system acquires images of an equivalent quality 40 times faster using only 1/5 the power per image.

MSAF imaging

Consider a MSAF system with an N -element virtual linear array. At the first step, a linear sub-array with N_t elements transmits an ultrasound pulse, and a linear sub-array with N_r elements receives the echo signals. At the next step, the two sub-apertures (transmit and receive) are moved by L elements and the process of transmission/reception is repeated. The principle scheme of data acquisition is illustrated in Fig. 1.

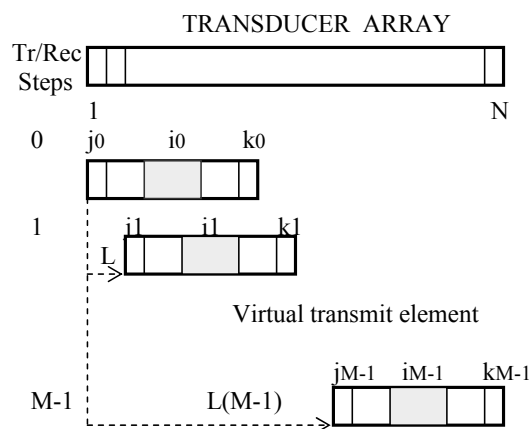


Fig. 1 Data acquisition in a MSAF imaging system

The number of transmissions needed to create a synthetic aperture equivalent to a virtual physical array with N elements is:

$$M = (N - N_r) / L + 1 \tag{1}$$

We assume that the signal processing is realized in the base band frequency domain, and $(M \times N_r)$ lines of the complex amplitude are stored in the computer memory after the quadrature detection. The image formation is carried out in two stages (Fig. 2).

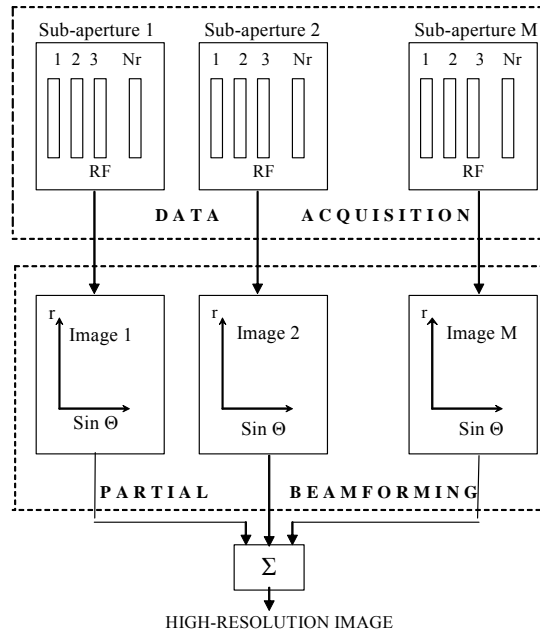


Fig. 2 Image formation in a MSAF imaging system

Firstly, the complex amplitude of each low-resolution image associated with the corresponding sub-aperture pair “transmitter-receiver” is obtained as a partial beamforming sum:

$$S_m(r, \theta) = \sum_{n=0}^{N_r-1} w_n U_{m,n}(t - \tau_{m,n}) \exp(j\Phi_{m,n}), \quad m = 1, \dots, M \quad (2)$$

where $S_m(r, \theta)$ is the complex amplitude focused at the point (r, θ) , $U_{m,n}$ is the complex amplitude received at the n^{th} element of the m^{th} receive sub-aperture, $\tau_{m,n}$ and $\Phi_{m,n}$ are the time delay and phase applied to the n^{th} element of the m^{th} receive sub-aperture during beamforming, w_n is the weighting coefficient applied to the n^{th} element of a receive sub-aperture. The phases $\Phi_{m,n}$ used in beamforming are evaluated as:

$$\Phi_{m,n} = 2\pi f_0 \tau_{m,n} \quad (3)$$

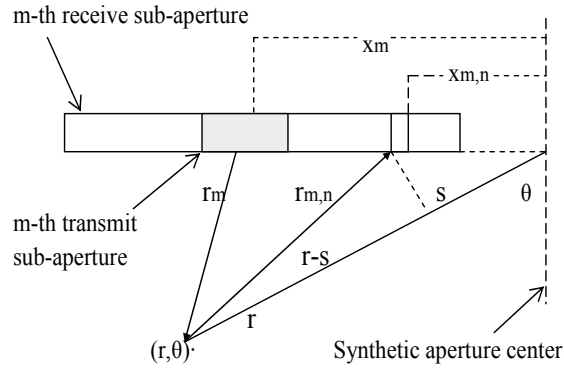
The parameter f_0 is the central frequency of a transducer. The complex amplitude of the final high-resolution image is formed as a sum:

$$S_{MSAF}(r, \theta) = \sum_{m=0}^{M-1} S_m(r, \theta) \quad (4)$$

The final B-images are obtained from (4) after the following signal processing – envelope detection, logarithmic compression, and scan conversion.

Partial beamforming

In the partial beamforming, the data recordings associated with a sub-aperture pair “transmitter-receiver” are focused at a point (r, θ) , where θ and r are the polar coordinates. We assume that the polar coordinate system is originated from the synthetic aperture center as is shown in Fig. 3.


 Fig. 3 The geometry of steering to point (r, θ)

The two-way time delay that must be applied to the n^{th} element of the m^{th} receive sub-aperture is:

$$\tau_{m,n} = \tau_m^{tr} + \tau_{m,n}^{rec} \quad (5)$$

where τ_m^{tr} is the one-way propagation time from the m^{th} transmit sub-aperture to the point (r, θ) , and $\tau_{m,n}^{rec}$ is the one-way propagation time from the point (r, θ) to the n^{th} element of the m^{th} receive sub-aperture. These time delays are evaluated as:

$$\tau_m^{tr} = \frac{r - \sqrt{r^2 + x_m^2 - 2rx_m \sin \theta}}{c} \quad (6)$$

$$\tau_{m,n}^{rec} = \frac{r - \sqrt{r^2 + x_{m,n}^2 - 2rx_{m,n} \sin \theta}}{c}$$

The position of a transmit sub-aperture (x_m) and the position of a receive sub-aperture element ($x_{m,n}$) about the synthetic aperture center are evaluated as:

$$x_m = (m - 1 - \frac{M - 1}{2}) \frac{L\lambda}{2}, \quad x_{m,n} = x_m + (n - 1 - \frac{N_r - 1}{2}) \frac{\lambda}{2} \quad (7)$$

where λ is the wave length corresponding to the central frequency f_0 of a transducer.

Spatial Sampling

The spatial sampling of the beam space must be consistent with the spatial Nyquist sampling criteria. According to [6], the spatial frequency bandwidth can be found using the effective aperture function of an imaging system. The effective aperture function of a MSAF system can be expressed as:

$$C = \sum_{m=1}^M A_m \otimes B_m, \quad A_m = [0, 0, \dots, a(i_m), \dots, 0, 0], \quad B_m = [0, \dots, 0, b_{m-N_r/2}, \dots, b_m, \dots, b_{m+N_r/2}, 0, \dots, 0] \quad (8)$$

where A_m is the full transmit aperture during the m^{th} firing, B_m is the full receive aperture during the m^{th} firing, $a(i_m) = 1$ is the weighting coefficient applied to the m^{th} transmit sub-aperture and $(b_{m-N_r/2}, b_{m-N_r/2+1}, \dots, b_m, \dots, b_{m+N_r/2-1}, b_{m+N_r/2})$ are weighting coefficients applied to the elements of the m^{th} receive sub-aperture, and \otimes is the convolution operator. The position of the m^{th} transmit/receive sub-aperture centers within a synthesized virtual array is

$i_m = N_r / 2 + L(m - 1) + 1$. The number of non-zero elements (N_{eff}) of the effective aperture function (8) can be valuated as:

$$N_{eff} = 2[N_r + L(M - 1)] - 2E(N_r / 2) - 1 \quad (9)$$

where $E(\cdot)$ is the integer number value. In case of odd values of N_r , the expression (9) takes the form:

$$(N_{eff})_{MSAF} = 2L(M - 1) + N_r \quad (10)$$

It must be noted that the effective aperture extent of the m^{th} sub-aperture pair “transmitter-receiver” is:

$$(N_{eff})_{LOW} = N_r \quad (11)$$

The Fourier transform of the effective aperture function gives the two-way radiation beam pattern of a MSAF system:

$$W(k) = \sum_{m=0}^{N_{eff}-1} C(k) \exp(-j \frac{2\pi}{N_{eff}} km) \quad (12)$$

The spatial frequency index k in (12) maps into the beam angle θ by:

$$\sin \theta = \frac{2k}{N_{eff}}, k = 0, \pm 1, \dots, \pm \frac{N_{eff} - 1}{2} \quad (13)$$

According to (13) the maximal sampling interval in θ for both, the low-resolution image and the high-resolution image, is defined by the following expressions:

$$(\Delta \sin \theta)_{high} = 2 / N_{eff}; (\Delta \sin \theta)_{low} = 2 / N_r \quad (14)$$

According to (14), the up sampling factor for a low-resolution image is:

$$K_{up} = 1 + D, \text{ where } D = 2L(M - 1) / N_r \quad (15)$$

The parameter D in (15) is the interpolation factor of low-resolution images.

Parameter optimization

In the MSAF imaging, the image quality depends on the size of a receive sub-aperture (N_r), the number of transmissions (M) and the sub-aperture spacing (L). The number of elements (N) in a synthetic aperture is determined by these parameters:

$$N = (M - 1)L + N_r \quad (16)$$

In most medical applications the image acquisition time is required to be extremely short to avoid problems caused by the tissue movement during the data acquisition. To satisfy such a requirement it is desirable to use only a few transmissions for image formation ($M < 10$). In this section, we assume that $M = 3, 5$ and 7 . The aim of parameter optimization is to find such a combination of parameters M, N_r and L that guarantees the same high quality of images as an equivalent PA imaging system with N transducer elements. The image quality is expressed in terms of the beam pattern parameters of a system - beam width ($\Delta\Theta$), the first side lobe peak (SLB-near) and the far side lobe peak (SLB-far). Firstly, the image quality is analyzed depending on the parameter sets (M, L, N_r). Secondly, the influence of such factors as the time

sampling rate and the signal-to-noise ratio (SNR) on the image quality is studied. In this section for the sake of simplification we assume that a transmit sub-aperture of a MSAF system consists of only one element, i.e. $N_t = 1$.

Beam pattern analysis. The effective aperture function and the corresponding two-way radiation beam pattern of a MSAF system is evaluated for parameter sets (N_r, M, L) that satisfy the following requirement:

$$(M - 1)L \leq N_r / 2 \tag{17}$$

The requirement (17) is needed to produce the effective aperture function that is unimodal and smoothly filled. Such an effective aperture function is formed by conventional PA systems [6]. The effective aperture and the corresponding two-way radiation beam pattern can be computed by the expressions (8) and (12), respectively.

In this study, four different receive sub-apertures with 15, 33, 63 and 129 elements are used for beam pattern analysis of a MSAF system. For the case of Chebyshev weighting, the beam parameters of these sub-apertures are presented in Table 1. This is a case of a single low-resolution image created by a single sub-aperture pair “transmitter-receiver”, i.e. when $M = 1$. It can be seen that the beam width ($\Delta\Theta^\circ$) varies in range from 14.76° (for a 15-element receive sub-aperture) to 1.7° (for a 129-element sub-aperture). For the case when $M > 1$, the beam parameters evaluated for various combination of (M, L, N_r) are presented in Tables 2-5.

Table 1. Beam parameters of a single receive sub-aperture

| Chebyshev window – (50dB) | | | |
|---------------------------|----------------------|---------------|--------------|
| N_r | $\Delta\Theta^\circ$ | SLB-near [dB] | SLB-far [dB] |
| 15 | 14.76 | -50 | -50 |
| 33 | 6.66 | -50 | -50 |
| 63 | 3.42 | -50 | -50 |
| 129 | 1.71 | -50 | -50 |

The beam parameters of a MSAF system that employs a 15-element receive sub-aperture are presented in Table 2. These results show that only a single set of system parameters ($N_r = 15, M = 3, L = 1$) enables to obtain a high-contrast MSAF image providing the side lobe level of -60dB. The beam width is reduced from 14.76° – for a low-resolution image ($M = 1$) to 12.8° – for a MSAF image, when three transmissions are used ($M = 3$) for synthetic aperture formation. The synthetic aperture of such a MSAF system is equivalent to an array of 17 elements ($N = 17$).

Table 2. Beam parameters of a MSAF system (15-element sub-aperture)

| Chebyshev window - (50dB) | | | | | | |
|---------------------------|----------|----------|-----------|----------------------|---------------|--------------|
| N_r | M | L | N | $\Delta\Theta^\circ$ | SLB-near [dB] | SLB-far [dB] |
| 15 | 3 | 1 | 17 | 12.8 | -60 | -60 |
| | | 2 | 19 | 9.63 | -30 | -50 |
| | | 3 | 21 | 7.20 | -20 | -50 |
| 5 | 1 | 19 | 10.4 | -41 | -64 | |
| 7 | 1 | 21 | 8.46 | -27 | -70 | |

The beam characteristics of a MSAF system that employs a 33-element receive sub-aperture are shown in Table 3. Beam pattern analysis shows that there are three appropriate sets of system parameters that make possible to obtain the high-contrast MSAF images. These optimal sets, $(N_r = 33, M = 3, L = 3)$, $(N_r = 33, M = 5, L = 2)$ and $(N_r = 33, M = 7, L = 1)$, provide the side lobe level of -60dB, -50dB and -70 dB, respectively. The second variant of system parameters $(N_r = 33, M = 5, L = 2)$, however, is more preferable providing the minimal beam width (4.95°). This variant of a MSAF system creates a synthetic aperture equivalent to a linear array with 41 elements ($N = 41$).

Table 3. Beam parameters of a MSAF system (33-element sub-aperture)

| N_r | M | L | N | Chebyshev window – (50dB) | | |
|----------|-----------|----------|-----------|---------------------------|---------------|--------------|
| | | | | $\Delta\theta^\circ$ | SLB-near [dB] | SLB-far [dB] |
| 33 | 3 | 1 | 35 | 6.48 | -52 | -60 |
| | | 2 | 37 | 5.94 | -62 | -60 |
| | | 3 | 39 | 5.31 | -60 | -50 |
| | | 4 | 41 | 4.59 | -35 | -50 |
| | | 5 | 43 | 4.05 | -26 | -50 |
| | | 7 | 47 | 3.15 | -20 | -50 |
| | | 5 | 1 | 1 | 37 | 6.12 |
| 2 | 41 | | | 4.95 | -50 | -50 |
| 3 | 45 | | | 3.96 | -28 | -50 |
| 4 | 49 | | | 3.24 | -21 | -50 |
| 7 | 1 | | | 39 | 5.67 | -70 |
| 7 | 2 | 1 | 39 | 5.67 | -70 | -70 |
| | | 2 | 45 | 4.14 | -30 | -50 |

The beam characteristics of a MSAF system, which employs a 63-element receive sub-aperture are shown in Table 4. These results show that there are three optimal parameter sets - $(N_r = 63, M = 3, L = 6)$, $(N_r = 63, M = 5, L = 4)$ and $(N_r = 63, M = 7, L = 2)$ that provide the relatively low level of side lobes (-50dB and below). The second parameter set $(N_r = 63, M = 5, L = 4)$, however, is the most preferable providing the minimal beam width (2.52°). This set of parameters creates a synthetic aperture equivalent to a linear array with 79 elements ($N = 79$).

For that variant of a MSAF system, the two-way beam pattern and the corresponding effective aperture function are plotted in Fig. 4 and Fig. 5, respectively. It can be seen that the side lobe level of -50dB is maintained in the full 90° – scan sector, and the effective aperture function is a limited convex function with only one maximum.

The beam characteristics of a MSAF system that employs a 129-element receive sub-aperture are shown in Table 5.

These numerical results show that there are three optimal parameter sets – $(N_r = 129, M = 3, L = 13)$, $(N_r = 129, M = 5, L = 8)$ and $(N_r = 129, M = 7, L = 6)$ that produce the relatively low level of side lobes (-50dB and below). The second parameter set $(N_r = 129, M = 5, L = 8)$, however, is the most preferable providing the minimal beam width (1.26°). This variant of parameters creates a synthetic aperture equivalent to a linear array with 161 elements ($N = 161$).

Table 4. Beam parameters of a MSAF system (63-element sub-aperture)

| N_r | M | L | N | Chebyshev window – (50dB) | | |
|-------|-----|----------|-----------|---------------------------|---------------|--------------|
| | | | | $\Delta\theta^\circ$ | SLB-near [dB] | SLB-far [dB] |
| 63 | 3 | 1 | 65 | 3.42 | -50 | -60 |
| | | 5 | 73 | 2.88 | -50 | -50 |
| | | 6 | 75 | 2.70 | -50 | -50 |
| | | 7 | 77 | 2.52 | -40.5 | -50 |
| | | 9 | 81 | 2.25 | -28 | -50 |
| 5 | 3 | 1 | 67 | 3.42 | -50 | -60 |
| | | 3 | 75 | 2.88 | -50 | -50 |
| | | 4 | 79 | 2.52 | -50 | -50 |
| | | 5 | 83 | 2.25 | -33 | -50 |
| | | 7 | 91 | 1.8 | -23 | -50 |
| 7 | 3 | 1 | 69 | 3.33 | -60 | -70 |
| | | 2 | 75 | 2.97 | -50 | -60 |
| | | 3 | 81 | 2.52 | -42 | -50 |
| | | 5 | 93 | 1.8 | -23 | -50 |

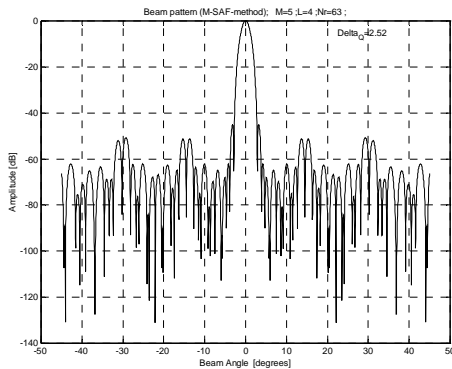


Fig. 4 Beam pattern of a MSAF system ($N_r = 63; M = 5; L = 4$)

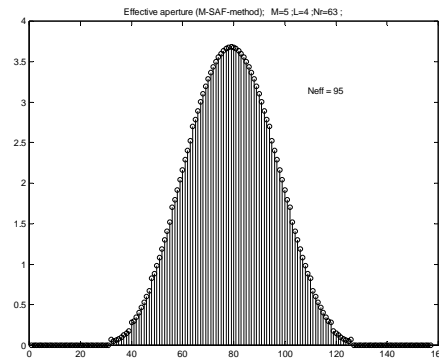


Fig. 5 Effective aperture of a MSAF system ($N_r = 63; M = 5; L = 4$)

Table 6 compares four optimal variants of a MSAF system with a corresponding equivalent PA system with the same number of phased array elements (N). It may be seen that both imaging systems, MSAF and PA, produce the nearly equivalent image quality but the MSAF systems utilize the smaller number of active transducer elements for image formation than the equivalent conventional PA systems ($N_r \ll N$).

Table 5. Beam parameters of a MSAF system
(129-element sub-aperture)

| N_r | M | L | N | Chebyshev window – (50dB) | | |
|-------|-----|-----------|------------|---------------------------|---------------|--------------|
| | | | | $\Delta\Theta^\circ$ | SLB-near [dB] | SLB-far [dB] |
| 129 | 3 | 1 | 131 | 1.71 | -50 | -70 |
| | | 9 | 147 | 1.53 | -50 | -50 |
| | | 13 | 155 | 1.35 | -50 | -50 |
| | | 17 | 163 | 1.17 | -30 | -50 |
| | | 25 | 179 | 0.90 | -20 | -50 |
| | | 31 | 191 | 0.72 | -16 | -50 |
| | 5 | 1 | 133 | 1.71 | -50 | -70 |
| | | 5 | 149 | 1.53 | -50 | -50 |
| | | 8 | 161 | 1.26 | -50 | -50 |
| | | 12 | 177 | 0.99 | -30 | -50 |
| | | 16 | 193 | 0.81 | -20 | -50 |
| | 7 | 1 | 135 | 1.71 | -50 | -70 |
| | | 3 | 147 | 1.53 | -60 | -50 |
| | | 6 | 165 | 1.26 | -50 | -50 |
| | | 10 | 189 | 0.90 | -30 | -50 |

Table 6. Parameters of MSAF and PA systems

| N_r | MSAF imaging system | | | | | PA imaging system | | |
|-------|---------------------|-----|-----|----------------------|----------|-------------------|----------------------|----------|
| | M | L | N | $\Delta\Theta^\circ$ | SLB [dB] | N | $\Delta\Theta^\circ$ | SLB [dB] |
| 15 | 3 | 1 | 17 | 12.87 | -60 | 17 | 13.0 | -50 |
| 33 | 5 | 2 | 41 | 4.95 | -50 | 41 | 5.31 | -50 |
| 63 | 5 | 4 | 79 | 2.52 | -50 | 79 | 2.79 | -50 |
| 129 | 5 | 8 | 161 | 1.26 | -50 | 161 | 1.35 | -50 |

Sampling rate. A 90° – sector scan of a point target is simulated in order to study the effect of the sampling rate on the quality of MSAF images. In simulations, the scan angle is incremented in steps of 0.45° from -45° to 45° . In case of a 33-element receive sub-aperture, the point target was located at 70 mm from the center of a synthetic aperture. In case of a 63-element receive sub-aperture, the distance to the point target was 200 mm. For each sub-aperture pair “transmitter-receiver”, all stored A-scans were base-band RF signals sampled at rate of 5 MHz, 10 MHz and 80 MHz. The beam width ($\Delta\Theta^\circ$) and the side lobe peak (SLB) of a MSAF system evaluated for three variants of sampling rate are presented in Table 7.

Table 7. Beam parameters for three variants of sampling rate

| Parameter | $F_s = 5$ MHz | | $F_s = 10$ MHz | | $F_s = 80$ MHz | | | |
|-----------|---------------|-----|----------------------|----------|----------------------|----------|----------------------|----------|
| | M | L | $\Delta\Theta^\circ$ | SLB [dB] | $\Delta\Theta^\circ$ | SLB [dB] | $\Delta\Theta^\circ$ | SLB [dB] |
| 33 | 3 | 3 | 5.34 | -25 | 5.33 | -35 | 5.31 | -45 |
| | 5 | 2 | 5.02 | -25 | 5.0 | -35 | 4.95 | -45 |
| | 7 | 1 | 5.71 | -25 | 5.69 | -35 | 5.62 | -45 |
| 63 | 3 | 6 | 2.69 | -28 | 2.63 | -40 | 2.57 | -47 |
| | 5 | 4 | 2.52 | -28 | 2.5 | -40 | 2.4 | -47 |
| | 7 | 2 | 2.92 | -28 | 2.89 | -40 | 2.81 | -47 |

The following parameters are used in simulations: center frequency – 3.5 MHz, pulse duration – $1\mu s$, SNR – 50dB, dynamic range – 50dB, weighting in receive – Chebyshev (-50dB). The

numerical results show that the sampling frequency must be chosen very carefully in order to guarantee the acceptable level of side lobes. In our case the sampling frequency higher than 80 MHz makes possible to ensure the near-optimum side lobe level of the MSAF beam pattern.

Resolution of closely-spaced point targets. Lateral resolution of a MSAF system is defined as a minimal distance (in scan angle) between two point targets at which separate registration is just distinguished on the display. A capability of a MSAF system to resolve two closely-spaced point targets with different reflectivity is studied by simulation. With this aim in mind, a sector scan of two closely-spaced point targets located at a distance of 200 mm is simulated in two stages. The first stage of simulation fits the case when both point targets have the identical reflectivity. In this simulation the SNR is assumed to be 20dB. The next stage of simulation fits the case when the point targets are not identical in reflectivity, and the difference in contrast is 5dB. In both cases it is assumed that the first target is located at the scan angle of 0° , the second target – at the scan angle of $\Delta\Theta$, where $\Delta\Theta$ is the beam width of a MSAF system. For a simulated system with parameters $N_r = 63$, $M = 5$ and $L = 4$, the beam width is $\Delta\Theta = 2.4^\circ$. The intensity of signals reflected from the closely-spaced targets is plotted in Fig. 6 – for identical targets in contrast and Fig. 7 – for different targets in contrast. It can be seen that two closely-spaced point targets are distinguishable only if the difference in intensity of their echo signals is insufficient.

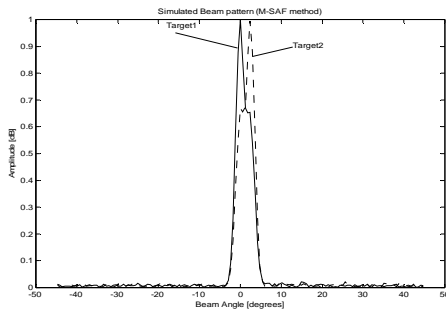


Fig. 6 Echoes from closely-spaced point targets ($\text{SNR}_1 = 20\text{dB}$; $\text{SNR}_2 = 20\text{dB}$)

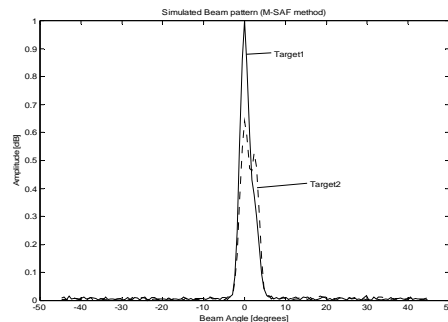


Fig. 7 Echoes from closely-spaced point targets ($\text{SNR}_1 = 20\text{dB}$; $\text{SNR}_2 = 15\text{dB}$)

Comparison analysis

The effectiveness of a MSAF imaging system is compared with that of an equivalent phased array imaging system. The comparison analysis is based on estimation of the following quality parameters – signal-to-noise ratio, consumed power per image, maximal intensity of a pulse, image acquisition time, beam width, and side lobe level. The system parameters used for estimation of the quality parameters are shown in Table 8.

In the conventional PA imaging, the minimum time required to form a single high-resolution image is proportional to the number of scan lines and the time needed to record the received signals during the transmission, i.e. $T_{PA} = 2N_{line}R_{max}/c$, and c is the velocity of sound. For $N_{line} = 201$ and $R_{max} = 200$ mm, the image acquisition time for a PA imaging system is $T_{PA} = 52$ ms. It means that a 201-line scan sector can be acquired at a rate of approximately 19 images per second. To increase the frame rate of a conventional PA scanner, the depth of view must be sacrificed by decreasing the size of the image, or the lateral resolution must be sacrificed by reducing the number of image lines. However, the same is not true for a MSAF imaging system, in which the image acquisition time is determined by the number of transmit

sub-apertures and equals $T_{MSAF} = 2MR_{\max} / c$. In that case, the process of image acquisition is speeded up ($T_{PA} / T_{MSAF} = N_{line} / M$) times. For $M = 5$, the image acquisition time for a MSAF system is $T_{MSAF} = 1.3$ ms. It means that a 201-line scan sector can be acquired at a rate of 770 images per second. It is 40 times faster than for a PA system.

Table 8. System parameters used for comparison analysis

| System parameters | PA System | | MSAF System | |
|--|------------|-------|-------------|-------|
| | Symbol | Value | Symbol | Value |
| # of array elements | N | 79 | N | 79 |
| # of elements in a transmit sub-aperture | N | 79 | N_t | 10 |
| # of elements in a receive sub-aperture | N | 79 | N_r | 63 |
| # of transmissions | - | - | M | 5 |
| Spacing between transmit/receive sub-apertures | - | - | L | 4 |
| Excitation pulse amplitude | | 1 | G | 8 |
| # of image lines | N_{line} | 201 | N_{line} | 201 |
| Maximal depth of imaging, [mm] | R_{\max} | 200 | R_{\max} | 200 |
| Angular sector, [°] | - | 90 | - | 90 |
| Weighting function | Chebyshev | | Chebyshev | |

In a conventional PA system, the transmit power per image is proportional to the number of array elements, the number of scan lines and the average power transmitted from each element, i.e. $P_{PA} = N \cdot N_{line} \cdot p_0$. In a MSAF system, a transmit sub-aperture with N_t defocused elements simulates a single virtual transmit element in order to increase the transmitted power. The amplitude of resulting transmission is increased in proportion to $\sqrt{N_t}$. To increase the transmit power the excitation amplitude is amplified G times (see Table 8). Therefore, for a MSAF system, the transmit power per image is $P_{MSAF} = M \cdot N_t \cdot G^2 p_0$. Compared to a PA system, the relative transmit power for a MSAF system is:

$$P_{MSAF} / P_{PA} = (M \cdot N_t \cdot G^2) / (N \cdot N_{line}) \tag{18}$$

For the system parameters shown in Table 8, the ratio (18) is 1/5. It means that the transmit energy per image is reduced 5 times compared to an equivalent PA system.

Similarly, the ratio of the maximum intensity in the transmit mode can be calculated for the two imaging systems system:

$$I_{MSAF} / I_{PA} = (G^2 N_t) / N^2 \tag{19}$$

For the system parameters shown in Table 8, the ratio (19) is 1/8. It means that in the transmit mode, the signal intensity is reduced 8 times compared to an equivalent PA system.

According to [6], in a conventional PA system, the signal is proportional to the number of array elements, i.e. $Signal \sim N$, while the noise is inversely proportional to the square root of the number of array elements, i.e. $Noise \sim 1/(N)^{1/2}$. Therefore, for a PA system the signal – to-noise ratio is $SNR_{PAF} \sim N^{3/2}$. Similarly, for a MSAF system we have: $Signal \sim G(N_t)^{1/2}$;

Noise $\sim 1/(N_r M)^{1/2}$; $SNR_{MSAF} \sim G(N_t M \cdot N_t)^{1/2}$. The relative SNR for a MSAF imaging system is:

$$SNR_{MSAF} / SNR_{PA} = G \sqrt{N_t N_r M} / \sqrt{N^3} \quad (20)$$

For the system parameters shown in Table 8, the ratio (20) is 0.65. Therefore, for a MSAF system, the losses in SNR are equal to -3.81 dB, compared to a PA system. Nevertheless, the signal-to-noise ratio in a MSAF system is within 6dB of an equivalent PA system.

Table 9 summarizes the comparison between the two imaging system. The comparison analysis shows that the MSAF system acquires images of equivalent image quality 40 times faster using only 1/5 the power per image.

Table 9. Quality parameters

| System Parameters | PAF system | MSAF system |
|---------------------------------|------------|-------------|
| Relative SNR | 0dB | -3.8dB |
| Relative power/image | 1 | 1/5 |
| Relative maximum Intensity | 1 | 1/8 |
| Relative image acquisition Time | 1 | 1/40 |
| Beam width | 2.79° | 2.52° |
| Side lobe level | -50dB | -50dB |

Finally, in the MSAF system, the common number of active elements used in each transmission/reception is sufficiently less ($N_t + N_r = 10 + 63 = 73$) than in an equivalent PA system ($N + N = 79 + 79 = 158$). Therefore, the complexity of the MSAF imaging system is reduced twice compared to an equivalent PA imaging system.

Conclusions

A technique for parameter analysis and optimization of a MSAF system is described. This technique can be useful at the stage of design of MSAF systems that employ only a few transmissions for image formation. The results obtained show that such system parameters as the number of transmit/receive sub-apertures, the number elements in each transmit/receive aperture, the spacing between sub-apertures, and the needed sampling rate can be optimized using the effective aperture approach. The choice of the optimal parameter set reduces to a trade-off of the narrowest beam against the lowest side lobe level. The comparison between the two imaging systems demonstrates that the MSAF system employing only a few ($M = 3, 5, 7$) pulse transmissions per image can produce images of equivalent image quality extremely faster than an equivalent conventional PA system. For most imaging applications, this acquisition speed can be fast enough to avoid problems caused by tissue movement during the image acquisition.

Acknowledgment

This work was financially supported by the Center of Excellence BIS21++, Contract 016639, and the Bulgarian National Science Fund, Grant MI-1506/05.

References

1. Behar V., D. Adam (2005). Optimization of a Sparse Synthetic Transmit Aperture Imaging with Coded Excitation and Frequency Division, *Ultrasonics*, 43, 777-788.
2. Cooley C., B. Robinson (1994). Synthetic Focus Imaging using Partial Data Sets, *Proceedings of 1994 Ultrasonics Symposium*, 1539-1542.
3. Frazier C., W. O'Brien (1998). Synthetic Aperture Techniques with a Virtual Source Element, *IEEE Trans. on Ultrasonics, Ferroelectrics Frequency Control*, 45, 196-207.
4. Karaman M., M. O'Donnell (1998). Sub-aperture Processing for Ultrasonic Imaging, *IEEE Trans. on Ultrasonics, Ferroelectrics Frequency Control*, 45, 126-135.
5. Karaman M., H. Bilge, M. O'Donnell (1998). Adaptive Multi-element Synthetic Aperture Imaging with Motion and Phase Aberration Correction, *IEEE Trans. on Ultrasonics, Ferroelectrics Frequency Control*, 45, 1077-1087.
6. Lockwood L., F. Foster (1995). Design of Sparse Array Imaging Systems, *Proceedings of IEEE Ultrasonics Symposium*, 1237-1243.
7. Nock L., G. Trahey (1992). Synthetic Receive Aperture Imaging with Phase Correction for Motion and for Tissue Inhomogeneities – Part I: Basic Principles, *IEEE Trans. on Ultrasonics, Ferroelectrics Frequency Control*, 39, 489-495.
8. Trahey G., L. Nock (1992). Synthetic Receive Aperture Imaging with Phase Correction for Motion and for Tissue Inhomogeneities – Part II: Effects of and Correction for Motion, *IEEE Trans. on Ultrasonics, Ferroelectrics Frequency Control*, 39 (4), 496-501.
9. Sverre H. et al. (1999). Method and Apparatus for Synthetic Transmit Aperture Imaging, USA Patent, N°5951479, Sept. 14.
10. Yao H. (1997). Synthetic Aperture Methods for Medical Ultrasonic Imaging, Hovedoppgave i Informatikk, Oslo University.
11. Ylitalo J., H. Ermert (1994). Ultrasound Synthetic Aperture Imaging: Monostatic Approach, *IEEE Trans. on Ultrasonics, Ferroelectrics Frequency Control*, 41, 333-339.
12. Ylitalo J. (1996). On the Signal-to-noise Ratio of a Synthetic Aperture Ultrasound Imaging Method, *European Journal of Ultrasound*, 3, 277-281.